JOURNAL OF CATALYSIS **163,** 232–244 (1996)
ARTICLE NO. 0324

Modification of Non-template Synthesized Ferrierite/ZSM-35 for *n*-Butene Skeletal Isomerization to Isobutylene

Wen-Qing Xu,* Yuan-Gen Yin,* Steven L. Suib,*,†,‡,[1] John C. Edwards,§ and Chi-Lin O'Young§

*U-60, Department of Chemistry, University of Connecticut, Storrs, Connecticut 06269; †Department of Chemical Engineering, University of Connecticut, Storrs, Connecticut 06269; ‡Institute of Materials Science, University of Connecticut, Storrs, Connecticut 06269; and §Texaco, Incorporated, Research and Development Center, P.O. Box 509, Beacon, New York 12508

Received July 13, 1995; revised May 13, 1996; accepted May 14, 1996

Non-template synthesized ferrierite/ZSM-35 has been successfully modified by removal of non-shape selective acid sites and lowering of the number of acid sites. Modified materials were extensively studied by XRD, FT-IR, NMR, XPS, ammonia TPD, and kinetic evaluations for skeletal isomerization of *n*-butene to isobutylene. Removal of non-shape selective acid sites from non-template synthesized ferrierite/ZSM-35 greatly suppresses butene dimerization reactions. These non-shape selective acid sites are located inside larger internal pores (as compared to the zeolitic pores) and on the surface of non-template synthesized ferrierite/ZSM-35 materials due to their lower crystallinity. Such non-shape selective acid sites were removed via framework dealumination of the surface with acid treatment. Lowering of the number of acid sites of non-template synthesized ferrierite/ZSM-35 decreases interactions of butene intermediates on adjacent acid sites and was achieved via framework dealumination by steaming. Steaming of non-template synthesized ferrierite/ZSM-35 at higher temperatures or higher steam pressures produces more dealumination and, accordingly, further lowering of the number of acid sites. The presence of Na^+/K^+ ions gives more resistance to framework dealumination during steaming and the same potential for removing strong and weak acid sites. However, steaming of ferrierite/ZSM-35 of hydrogen form leads to removal of greater amounts of strong acid sites than weak acid sites. Studies have shown that steaming of non-template synthesized ferrierite/ZSM-35 of Na^+/K^+ forms followed by NH_4^+ ion exchange and acid washing is an effective modification procedure. Catalytic performances for such modified materials are very similar to those for template-synthesized materials, with respects to yields, selectivities, and catalytic stability.

I. INTRODUCTION

Methyl *t*-butyl ether (MTBE) is currently used as a major booster of octane number of gasoline (1). Isobutylene is an important raw material for production of MTBE. However, isobutylene supply is limited by the capacity of catalytic cracking of petroleum. In the effort to find an alternative source for isobutylene, selective skeletal isomerization of *n*-butene is of a great practical significance.

Medium pore zeolite ZSM-5 (5.3×5.6, 5.1×5.5 Å) has been widely used as a shape selective catalyst in petrochemical industries for isomerization of ortho- and meso-xylenes to para-xylene, conversion of methanol to gasoline, and conversion of methanol to olefins. However, it becomes non-shape selective for isomerization of *n*-butene (small molecule) to isobutylene, mainly due to severe dimerization of butene and subsequent cracking. Our efforts have been devoted to weakening of the acidity of ZSM-5 and ZSM-11 zeolites by substitution of aluminum with boron (2–5). Boron substitution weakens the strength of acid sites, which leads to significant suppression of dimerization of butene. However, pore sizes of boron-substituted ZSM-5 and ZSM-11 zeolites are still large enough so that dimerization reactions cannot be effectively suppressed.

Our research has shown that zeolites of smaller pores such as ferrierite/ZSM-35 (6–8). ZSM-23 (9), and θ-1/ZSM-22 (10) are superior shape selective catalysts for skeletal isomerization of *n*-butene with excellent yield and selectivity to isobutylene. Ferrierite/ZSM-35 has an orthorhombic framework (11) containing one-dimensional channels of 10-member rings (4.2×5.4 Å) and one-dimensional channels of 8-member rings (3.5×4.8 Å). These two kinds of channels are perpendicularly intersected. The 8-member ring channels contain spherical cavities with a size of about 6 to 7 Å.

As high as 36% yields and near 90% selectivities to isobutylene have been achieved with ferrierite/ZSM-35 catalysts (6). Coke deposits on ferrierite/ZSM-35 at an initial stage of reaction leads to poisoning of strong acid sites and partial blocking of channels. Therefore, dimerization reactions of butene are greatly suppressed due to poisoning of strong acid sites and shrinkage of the space around acid sites. Catalytic performance for ferrierite/ZSM-35 catalysts also depends on the crystallinity of these materials (8). Higher crystallinity leads to better shape selectivity for reactions of *n*-butene skeletal isomerization to isobutylene.

[1] To whom all correspondence should be addressed.

0021-9517/96 $18.00

Ferrierite/ZSM-35 has been successfully synthesized by several hydrothermal methods. The organic templates involved in the preparation of ferrierite are alkene-polyamines (12), 1,4-diaminocyclohexane (13), cholin (14), piperidine (15), pyrrolidine (16, 17), and cyclohexylamine (18). Without any organic template, ferrierite/ZSM-35 can only be synthesized under conditions of stirring. The resulting product has a narrow range of silicon to aluminum ratios centered approximately at nine (19).

Template-synthesized (using pyrrolidine) and non-template synthesized (supplied by Texaco, Inc.) ferrierite/ZSM-35 materials were characterized by X-ray diffraction (XRD), nuclear magnetic resonance (NMR) spectroscopy, Fourier-transform infrared (FTIR) spectroscopy, X-ray photoelectron (XPS) spectroscopy, and pore size distributions (8). It has been concluded that template-synthesized ferrierite/ZSM-35 materials have higher crystallinity than non-template synthesized ferrierite/ZSM-35 materials. Ferrierite/ZSM-35 of poorer crystallinity has more acid sites which are located inside larger pores, as compared to zeolitic pores, or on the external surface. Such acid sites have enough space for dimerization of butene molecules. Therefore, non-template synthesized ferrierite/ZSM-35 materials are not as shape selective for *n*-butene skeletal isomerization to isobutylene as template-synthesized ferrierite/ZSM-35 materials (8).

However, synthesis of ferrierite/ZSM-35 using pyrrolidine as a structure-directing template is an expensive process. This gives an economic initiative for further modification of non-template synthesized ferrierite/ZSM-35 for skeletal isomerization of *n*-butene to isobutylene. Removal of acid sites located on the external surface or large internal pores of non-template synthesized ferrierite/ZSM-35 materials will suppress dimerization of butene molecules. Lowering of the number of acid sites in ferrierite/ZSM-35 may decrease the possibility for interactions of two butene intermediates on adjacent acid sites, so that selectivity to isobutylene would be improved.

Modification of non-template synthesized ferrierite/ZSM-35 in this study involves steaming ferrierite/ZSM-35 of sodium/potassium and hydrogen forms at different temperatures and steam pressures, acid-washing ferrierite/ZSM-35, and steaming followed by acid-washing. Steaming is used to remove aluminum ions from the framework of ferrierite/ZSM-35 to lower the number of acid sites. Acid washing is used to remove aluminum ions on the external surface of zeolite particles, i.e., it removes non-shape selective acid sites so as to suppress dimerization or oligomerization of butene. Steaming followed by acid washing has been proven to be a valid method to modify non-template synthesized ferrierite/ZSM-35 for butene skeletal isomerization. Excellent yields of isobutylene (40%), selectivities to isobutylene (>90%), and stability (with respect to activity and selectivity) have been achieved.

II. EXPERIMENTAL SECTION

A. Preparation of Catalysts

A non-template synthesized Na/K-FER having a silicon to aluminum ratio of 8.8 was received from Texaco, Inc. It contains 1.11 wt% of Na^+ ions and 4.65 wt% of K^+ ions. Ferrierite/ZSM-35 of an ammonium form, NH_4-FER, was obtained by ion exchange of Na/K-FER two times with 1 *M* aqueous solution of ammonium nitrate at 353 K. This NH_4-FER sample still contains 0.12 wt% of K^+ and less than 0.05 wt% of Na^+ ions. NH_4-FER sample was then deaminated to H-FER by calcination of NH_4-FER at 823 K under a flow of nitrogen gas.

Both H-FER and Na/K-FER samples were steamed at different temperatures (823, 923, and 1023 K) and different pressures of water vapor (6.67×10^3, 1.33×10^4, and 2.66×10^4 Pa). Different pressures of water vapor were controlled by bubbling a stream of nitrogen gas into two water containers (in series) which were maintained at high and low temperatures, respectively. The temperature for the high-temperature water container is 15 K higher than that for the low-temperature one. This stream of nitrogen which was water vapor-saturated in the low-temperature water container was then introduced into a quartz reactor containing about 2 g of ferrierite materials. Steaming was carried out for 2.5 h.

Sample names for the steamed ferrierite/ZSM-35 materials are listed in Table 1. The character *S* which means "steaming" is followed by a double digit number. The first digit is assigned to the steaming temperature, i.e., 1, 2, and 3 correspond to 823, 923, and 1023 K, respectively. The second digit is assigned to the water vapor pressure during steaming, i.e., 1, 2, and 3 correspond to 6.67×10^3, 1.33×10^4, and 2.66×10^4 Pa, respectively. Names for these steamed ferrierite/ZSM-35 materials from H-FER are prefixed with H. Steamed Na/K-FER materials were also ion exchanged to their ammonium form, as described in the last paragraph. Names for these steamed ferrierite/ZSM-35 materials of ammonium form (from their steamed alkali forms) are prefixed by NH_4.

Ferrierite/ZSM-35 materials were also washed by different concentrations of HCl or HNO_3 solutions. This kind of acid washing was carried out at a temperature of 253 K

TABLE 1

Nomenclature of Steamed Ferrierite/ZSM-35 Samples

	Steam Pressure, Pa		
Temperature, K	6.67×10^3	1.33×10^4	2.66×10^4
823	S11	S12	S13
923	S21	S22	S23
1023	S31	S32	S33

for 12 h. Typically, 100 cm^3 of 1.4 *M* HNO_3 aqueous solution were used to wash 1 g of H-FER sample. Names for such acid-washed samples are suffixed by A, for example, H-FER-A.

B. Characterization

X-ray diffraction (XRD) experiments were done on a Scintag Model XDS 2000 diffractometer with a monochromatic X-ray beam and scintillator. Samples were mounted on a glass plate that remained horizontal during all experiments. A beam voltage of 45 kV and a current of 40 mA were used with Cu$K\alpha$ radiation. Software of "LATCON" and "INDEX" in this XRD instrument was used to calculate lattice parameters of ferrierite/ZSM-35 materials.

Fourier transform infrared (FTIR) experiments were done on a Nicolet 750 spectrometer at a resolution of 4 cm^{-1} by using either KBr pellets or self-supporting wafers. Pyridine chemisorption experiments were done on self-supported wafers in an *in situ* IR cell. The sample was dehydrated at 773 K for 5 h under a vacuum of 1.33×10^{-3} Pa followed by adsorption of purified pyridine vapor at room temperature for 15 min. The system was then evacuated at 423 K overnight to remove physisorbed pyridine and an infrared spectrum was recorded.

Magic angle spinning nuclear magnetic resonance (MAS NMR) spectroscopy data were acquired on a Varian Unity-300 spectrometer. ^1H and ^{29}Si spectra were obtained at resonance frequencies of 300 and 59.9 MHz, respectively, using a Doty Scientific 7-mm CP/MAS probe. The ^{27}Al spectra were acquired with a Chemmagnetics 7-mm CP/MAS probe at a resonance of 78.8 MHz. A 10° tip angle in conjunction with a 1-s recycle delay was employed to obtain both the ^1H and ^{27}Al spectra, while a 30° tip angle and an 8-s recycle delay were used to obtain the ^{29}Si spectra. The ^1H and ^{29}Si spectra are referenced to tetramethylsilane (TMS) and the ^{27}Al spectra are referenced to crystalline $KAl(SO_4)_2$.

X-ray photoelectron spectroscopy (XPS) experiments were done on a Leybold Heraeus Model LHS 10 spectrometer with an EA10 hemispherical analyzer detector. The spectrometer was calibrated to both the Au $4f_{7/2}$ transition at 83.8 eV and the Cu $2p_{3/2}$ transition at 923.4 eV. Both Mg and Al$K\alpha$ radiation were used. Samples were loaded on indium foil, and the C 1*s* signal was set at 284.6 eV for adventitious carbon.

Temperature-programmed desorption (TPD) experiments were done on a TPD apparatus described previously (2, 20). The sample was first heated from room temperature to 823 K at a ramping rate of 15 K/min and then soaked at 823 K for 1 h under a flow of 30 cm^3/min ultrapure helium. The system was then cooled to 373 K over 100 min. Ammonia was then flowed over the sample for 30 min. The sample was then purged with helium for 40 min in order to eliminate physisorbed species. The temperature was ramped at 15 K/min from 373 to 883 K and TPD data were acquired.

Compositions of ferrierite/ZSM-35 materials were analyzed by the methods of inductively coupled plasma (ICP). ICP analysis were conducted on a Perkin-Elmer ICP/5500 spectrometer. Contents of silicon, aluminum, sodium, and potassium were determined for these ferrierite/ZSM-35 materials.

C. Catalysis

Butene isomerization reactions were carried out in a microreactor loaded with 140 mg of zeolite catalysts. The reactor was heated from room temperature to 823 K at a ramping rate of 15 K/min in a flow of nitrogen of 60 cm^3/min. The temperature of the reactor was maintained at 823 K for 30 min in order to obtain zeolite catalysts of hydrogen form from an ammonium form. Then the reactor was cooled to 693 K for 20 min. The reactor was then maintained at 693 K and the nitrogen flow was switched to a mixture of but-1-ene and nitrogen (1 : 1 molar ratio). Flow rates of both but-1-ene and nitrogen were all controlled at 5 cm^3/min. Reaction products were analyzed every hour after 10 min time on stream with a Hewlett Packard 5890 Series II GC. This GC was equipped with a GS-Alumina capillary column (J&W Scientific) and a thermal conductivity detector (TCD). Literature values for TCD response coefficients were used for calibration (21, 22).

III. RESULTS

A. ^{29}Si and ^{27}Al Magic Angle Spinning Nuclear Magnetic Resonance Spectroscopy

Figure 1 shows the ^{29}Si single-pulse MAS NMR spectra for ferrierite/ZSM-35 materials. Q_4 resonances of $Si(OSi)_4$ were clearly observed for the fresh sample, H-FER, at −109 and −113 ppm, Fig. 1a. The resonance at −105 ppm for Q_4 $Si(OSi)_3(OAl)$ was also observed for H-FER. However, the resonance of Q_4 $Si(OSi)_2(OAl)_2$ at −100 ppm was not detectable due to its relatively high ratio of silicon to aluminum (8.8). Steamed ferrierite/ZSM-35 (H-S22) and its acid-washed product (H-S22-A) have very similar ^{29}Si SP/MAS NMR spectra, Figs. 1c and 1e. Q_4 $Si(OSi)_4$ resonances are all observed for these two samples at −111 and −114 ppm. However, the intensity for the resonance at −105 ppm for Q_4 $Si(SiO)_3(OAl)$ is decreased by a factor of 50%, as compared to that for H-FER (Fig. 1a). In addition, a shoulder at −116 ppm is also observed in ^{29}Si SP/MAS NMR spectra for both H-S22 and H-22-A. Such a resonance at −116 ppm is probably due to amorphous siliceous materials in both steamed samples (H-S22 and H-S22-A).

^{29}Si cross polarization MAS NMR spectra for both H-S22 and H-S22-A were also acquired, Fig. 1b and Fig. 1d, respectively. Two resonances at −102 and −108 ppm are observed

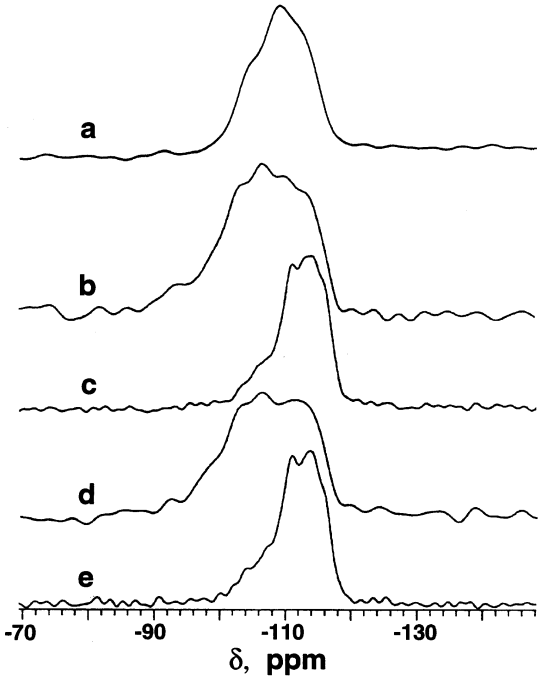

FIG. 1. ^{29}Si MAS NMR spectra for fresh and steamed non-template synthesized ferrierite/ZSM-35 materials. (a) H-FER (single pulse), (b) H-S22 (cross-polarization), (c) H-S22 (single pulse), (d) H-S22-A (cross-polarization), (e) H-S22-A (single pulse).

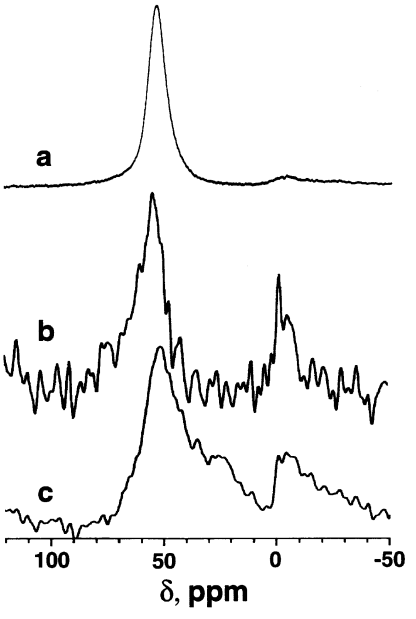

FIG. 2. ^{27}Al single-pulse MAS NMR spectra for fresh and steamed non-template synthesized ferrierite/ZSM-35 materials. (a) H-FER, (b) H-S22, (c) H-S22-A.

and their intensities are as strong as resonances at −111 and −114 ppm. These two extra resonances in CP/MAS NMR spectra, as compared to ^{29}Si SP/MAS NMR spectra, are due to defect silicon sites rather than Q_4 $Si(OSi)_3(OAl)$.

^{27}Al single pulse MAS NMR spectra for H-FER, H-S22, and H-S22-A are shown in Fig. 2a, Fig. 2b, and Fig. 2c, respectively. Tetrahedral Al^{3+} ions in the framework of ferrierite/ZSM-35 have been observed for all three samples by a resonance at about 54 ppm. The resonance at −2 ppm which is due to extraframework Al^{3+} ions in an octahedral environment is very weak for the fresh sample (H-FER) in Fig. 2a, about 4% of peak intensity at 54 ppm. However, the intensity for the resonance at −2 ppm is greatly enhanced for sample H-S22. The ratio of intensity of the resonance at 54 ppm to that at −2 ppm for H-S22 is about 9 : 5. H-S22-A obtained by acid washing H-S22 yields a weaker resonance at −2 ppm (octahedral Al^{3+}), as compared to that for H-S22. At the same time, there appears a resonance at about 25 ppm which may be due to 5 coordinate Al^{3+} ions. The ratio of the resonance for framework Al^{3+} ions (54 ppm) to the resonances for extraframework Al^{3+} ions (both peaks at −2 and 25 ppm) is about 4 : 3 for the acid-washed sample, H-S22-A.

B. Fourier-Transform Infrared Spectroscopy

Infrared spectra in the region of 3900 cm^{-1} to 3400 cm^{-1} for different steamed ferrierite/ZSM-35 samples (H-S series) are shown in Fig. 3. For the fresh ferrierite/ZSM-35 sample (Fig. 3a), two infrared bands occur at 3609 cm^{-1} and 3742 cm^{-1}. The IR band at 3609 cm^{-1} is due to hydroxyl groups which correspond to strong Brønsted acid sites and are also associated with silicon and aluminum ions. The IR band at 3742 cm^{-1} corresponds to terminal silanol groups. It is difficult to observe other IR bands in the region of 3742 cm^{-1} to 3609 cm^{-1}. However, several new IR bands appear between these two original IR bands

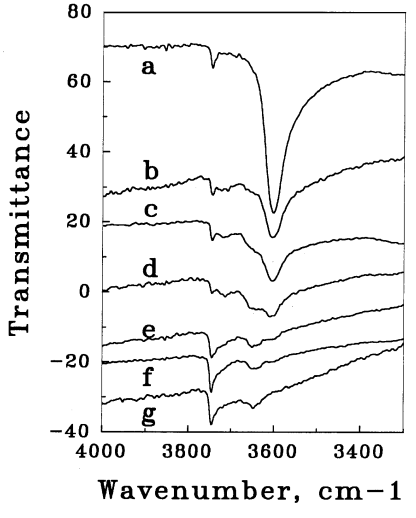

FIG. 3. FT-IR spectra for fresh and steamed non-template synthesized ferrierite/ZSM-35 materials. (a) H-FER, (b) H-S11, (c) H-S12, (d) H-S13, (e) H-S31, (f) H-S32, (g) H-S33.

TABLE 2

The Variation of IR Peak Areas at 3740 cm^{-1} and 3609 cm^{-1} for Ferrierite/ZSM-35 Materials Steamed at Different Conditions

Sample	Temperature, K	Pressure, Pa	A_{3742}	A_{3609}
H-FER	Fresh	Fresh	0.50	31.2
H-S11	823	6.67×10^3	0.49	13.4
H-S12	823	1.33×10^4	0.48	12.6
H-S13	823	2.66×10^4	0.45	7.00
H-S31	1023	6.67×10^3	0.71	2.74
H-S32	1023	1.33×10^4	0.79	2.27
H-S33	1023	2.66×10^4	1.18	1.87

(3742 cm^{-1} and 3609 cm^{-1}) after the fresh H-FER sample was steamed at 823 K for 2.5 h under different steam pressure, as shown in Fig. 3b–d (corresponding to 6.67×10^3, 1.33×10^4, and 2.66×10^4 Pa, respectively). The IR band at 3609 cm^{-1} moves to about 3649 cm^{-1} after steaming. Such new IR bands become more and more intense as the steam pressure increases, while intensities of the IR bands at 3609 cm^{-1} decrease as the steam pressure increases, Table 2. Data in Table 2 also suggest that peak areas of IR bands at 3742 cm^{-1} are constant for three ferrierite/ZSM-35 samples (H-S11, H-S12, and H-S13) which were steamed at 823 K. The IR band at 3609 cm^{-1} for ferrierite/ZSM-35 samples which were steamed at 1023 K gradually fades away as the steam pressure increases from 6.67×10^3 to 1.33×10^4, and 2.66×10^4 Pa, corresponding to Fig. 3e–g, respectively. Data in Table 2 show that the peak areas corresponding to Brønsted acid sites are decreased as steam pressure increases. The peak areas for terminal silanol groups (3742 cm^{-1}) are increased as steam pressure increases.

Pyridine chemisorption on these steamed ferrierite/ZSM-35 materials was also studied by FT-IR spectroscopy. Observed IR bands at 1540 cm^{-1} and 1460 cm^{-1} are due to pyridine molecules adsorbed on Brønsted and Lewis acid sites, respectively. Data in Table 3 illustrate the variation of IR peak areas at 1540 cm^{-1} and 1460 cm^{-1} with different steaming conditions. Steaming at 823 K for 2.5 h, the peak area of 1540 cm^{-1} decreases and that of 1460 cm^{-1} increase, as the steam pressure increases from 6.67×10^3 to 2.66×10^4 Pa. This indicates that some Brønsted acid sites are converted to Lewis acid sites due to the steaming. Steaming at a higher temperature (at 1023 K) produces steamed ferrierite/ZSM-35 materials containing least amounts of acid sites including both Brønsted and Lewis acidity. Both peak areas at 1540 cm^{-1} and 1460 cm^{-1} are relatively constant as a function of steam pressure. Different steam pressures at 1023 K did not produce different ferrierite/ZSM-35 materials as regards acidity. Perhaps pyridine chemisorption is not sensitive enough to detect differences in acidity caused by varying the steam pressure from 6.67×10^3 to 2.66×10^4 Pa at such a high temperature (1023 K).

TABLE 3

The Variation of IR Peak Areas at 1540 cm^{-1} and 1450 cm^{-1} for Ferrierite/ZSM-35 Materials Steamed at Different Conditions

Sample	Temperature, K	Pressure, Pa	A_{1540}	A_{1460}
H-FER	Fresh	Fresh	2.74	0.60
H-S11	823	6.67×10^3	1.46	0.81
H-S12	823	1.33×10^4	1.28	0.87
H-S13	823	2.66×10^4	1.09	0.93
H-S31	1023	6.67×10^3	0.56	0.64
H-S32	1023	1.33×10^4	0.62	0.63
H-S33	1023	2.66×10^4	0.60	0.52

C. Temperature-Programmed Desorption

Temperature-programmed desorption of ammonia allows quantitative determination of the amount and strength of acid sites on steamed ferrierite/ZSM-35 materials. Figure 4 shows ammonia TPD results for ferrierite/ZSM-35 samples which were obtained by steaming H-FER sample at different temperatures and different steam pressures. Desorption of ammonia via increasing the temperature for fresh ferrierite/ZSM-35 samples (Fig. 4a) shows two peaks at 471 and 732 K, respectively. The amount of desorbed ammonia at high temperature (732 K) is 1.19 times greater than that at low temperature (471 K). Steaming of

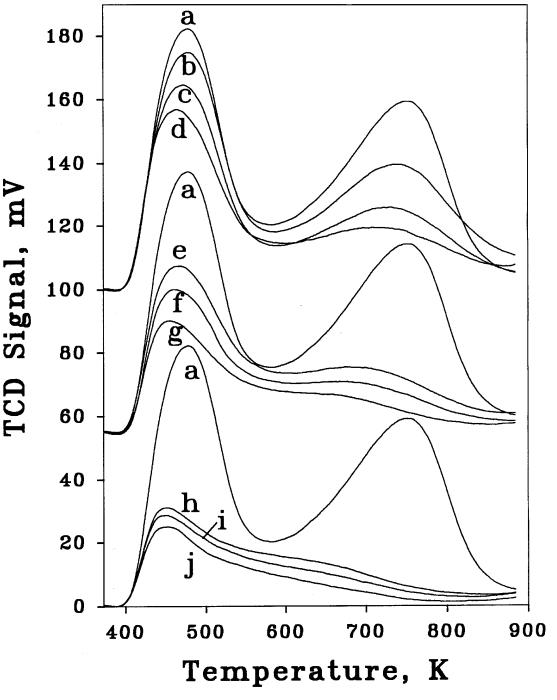

FIG. 4. Temperature-programmed desorption of ammonia for fresh and steamed H-FER materials. (a) H-FER, (b) H-S11, (c) H-S12, (d) H-S13, (e) H-S21, (f) H-S22, (g) H-S23, (h) H-S31, (i) H-S32, (j) H-S33.

H-FER at very mild conditions (823 K and 6.67×10^3 Pa) has already led to a significant decrease in the intensity of ammonia desorption, Fig. 4b. Steaming of H-FER with higher steam pressures (1.33×10^4 and 2.66×10^4 Pa) at 823 K produces a greater decrease in the amount of desorbed ammonia (Figs. 2c and 4d). The amount of desorbed ammonia for ferrierite/ZSM-35 materials becomes less and less as the steaming temperature increases from 823 K to 923 K (Fig. 4e–g) and 1023 K (Fig. 4h–j). At the same time, using higher steam pressure also yields steamed ferrierite/ZSM-35 materials containing less acidic sites. Quantitative data of Table 4 show that H-S33 which was obtained by steaming H-FER at 1023 K and 2.66×10^4 Pa for 2.5 h only has about 22.5% of the ammonia uptake for the fresh H-FER sample. Table 4 also shows that the decrease in ammonia uptake for the high-temperature peak is greater than that for the low-temperature peak.

Figure 5 shows the results of ammonia TPD for ferrierite/ZSM-35 materials which were obtained by steaming Na/K-FER at different temperatures and steam pressures followed by ion exchange of the steamed Na/K-FER materials with NH_4^+ ions. Steaming of Na/K-FER at 823 K (Figs. 5b–d) and 923 K (Figs. 5e–g) produces similar ferrierite/ZSM-35 materials as long as the applied steam pressures (6.67×10^3, 1.33×10^4, and 2.66×10^4 Pa) are the same. However, steaming at 1023 K has led to more significant decreases in ammonia uptake (Figs. 5h–j) as compared to those at 823 or 923 K. In addition, higher steam pressures enhanced the decrease in ammonia uptake. Quantitative data for ammonia uptake are also listed in Table 4. Comparison of the ammonia uptake with those for samples H-S11 to H-S33 suggests that the existence of alkali ions (Na^+ and K^+) gives ferrierite/ZSM-35 frameworks that are more resistant to dealumination with steaming. The decrease in ammonia uptake for samples NH_4-S11 to NH_4-S33 is evenly distributed in both high- and low-temperature peaks of ammonia desorption.

TABLE 4

Percentages of Ammonia Uptakes for Steamed Ferrierite/ZSM-35 Materials on the Basis of 5.08 NH_3 Molecules per Unit Cell for the Fresh Sample, H-FER

Sample	Percentage	H/L[a]	Sample	Percentage	H/L[a]
H-S11	78.0	0.80	NH_4-S11	94.5	1.18
H-S12	66.4	0.75	NH_4-S12	89.3	1.20
H-S13	56.5	0.72	NH_4-S13	87.7	1.22
H-S21	57.6	0.72	NH_4-S21	94.6	1.20
H-S22	44.8	0.66	NH_4-S22	89.9	1.18
H-S23	33.7	0.61	NH_4-S23	88.8	1.21
H-S31	34.0	0.61	NH_4-S31	87.6	1.14
H-S32	29.3	0.55	NH_4-S32	78.5	1.18
H-S33	22.5	0.41	NH_4-S33	54.4	1.16

[a] Ratio of ammonia uptake at high desorption temperature to that at low temperature (1.19 for the fresh sample, H-FER).

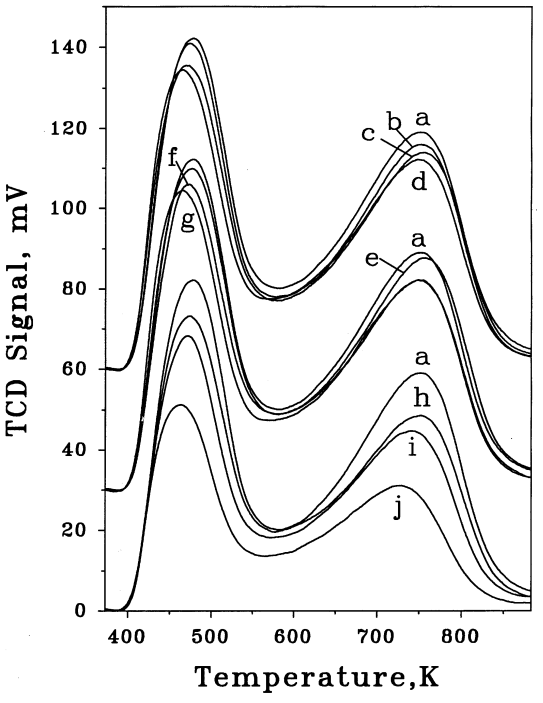

FIG. 5. Temperature-programmed desorption of ammonia for fresh and steamed Na/K-FER materials followed by NH_4^+ ion exchange. (a) H-FER, (b) H-S11, (c) H-S12, (d) H-S13, (e) H-S21, (f) H-S22, (g) H-S23, (h) H-S31, (i) H-S32, (j) H-S33.

Washing of H-FER with 1.4 *M* HNO_3 at 353 K for 12 h yielded sample H-FER-A. Samples H-FER and H-FER-A show similar ammonia uptake for the low-temperature desorption peak except that there is a slight temperature shift from 471 to 457 K. However, the high-temperature desorption peak for sample H-FER-A is about 9.1% less than that for sample H-FER. In other words, sample H-FER-A has a total ammonia uptake which is about 4.9% less than the fresh sample H-FER.

About 5% more acid sites were generated for sample H-S22-A which was obtained by washing sample H-S22 with 1.4 *M* HNO_3 at 353 K for 12 h. These extra acid sites were also generated by ion exchange of H-S22 with 1 *M* NH_4NO_3 at 353 K for 12 h.

D. X-Ray Photoelectron Spectroscopy

Surface compositions of ferrierite/ZSM-35 materials were analyzed by the method of X-ray photoelectron spectroscopy. Both the Si 2*p* signal at about 102.5 eV and the Al 2*p* signal at about 74.6 eV were used to semi-quantitatively calculate the ratio of silicon to aluminum on the surface. XPS results showed that the ratio of silicon to aluminum was 6.0 for the surface of the fresh ferrierite sample (H-FER). It was then increased from 6.0 for H-FER to 7.8 for H-FER-A (obtained by washing H-FER with 1.4 *M* HNO_3 for 12 h at 353 K). Steaming of H-FER at 923 K and 1.33×10^4 Pa followed by acid washing yielded

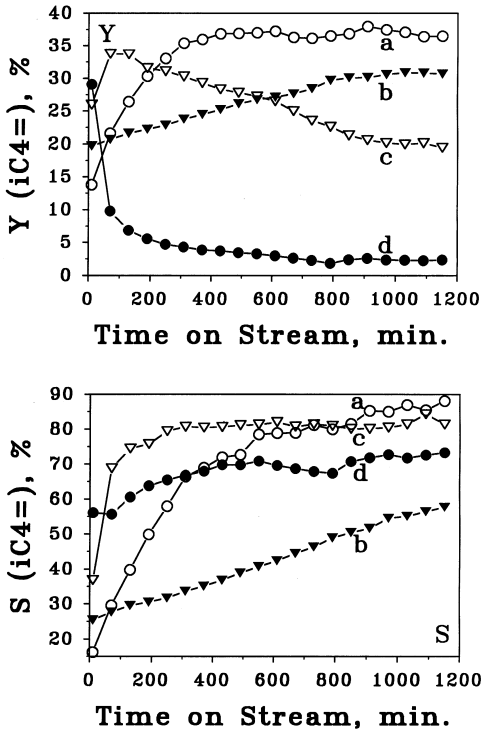

FIG. 6. Yields (Y) and selectivities (S) for *n*-butene skeletal isomerization at a temperature of 693 K and a 1-butene space velocity of 5.34 WHSV (weight hour space velocity) on fresh and steamed ferrierite/ZSM-35 materials. (a) H-FER, (b) H-S11, (c) H-S22, (d) H-S33.

sample H-S22-A. XPS analysis showed that the ratio of silicon to aluminum for the surface of H-S22-A was about 8.0, very similar to that for H-FER-A (7.8).

E. Catalytic Skeletal Isomerization of n-Butene to Isobutylene

1. Steaming of H-FER materials. Figure 6 presents yields and selectivities for *n*-butene skeletal isomerization to isobutylene on non-template synthesized ferrierite/ZSM-35 materials and their steamed derivatives. Yields of isobutylene are as high as 36% and selectivities as high as 90% for H-FER catalysts at steady state, as shown in Fig. 6Y and Fig. 6S. However, yields of 14% and selectivities of 16% for isobutylene are observed at a time on stream (TOS) of 10 min. Yields and selectivities to isobutylene are then gradually increased until steady state is reached as the TOS increases. By-products consist mainly of C_2 to C_8 olefins due to dimerization of *n*-butene followed by cracking. However, at the beginning of the reaction (TOS less than 10 min), about 10% of the products consist of ethane, propane, and butanes. After the first hour of TOS, the amount of light alkanes in the products reduces to less than 2%.

Sample H-S11 was produced by steaming of non-template ferrierite/ZSM-35 materials at 823 K and 6.67×10^3 Pa of steam. At a TOS less than 1 h, both yields and selectivities for isobutylene are greater than those for the fresh sample (H-FER). However, yields and selectivities for isobutylene are significantly smaller than those for the fresh sample (H-FER) when the TOS is longer than 1 h. H-S22 and H-S33 were obtained by steaming H-FER at 923 K and 1.33×10^4 Pa and at 1023 K and 2.66×10^4 Pa, respectively. Yields of isobutylene for H-S22 are greater than those for the fresh sample in the first 3 h TOS. They are smaller than those for H-FER after the TOS is longer than 3 h. Improvement of the selectivity to isobutylene for this catalyst (H-S22) can persist up to 11 h TOS. However, H-S33 only shows a greater yield (29%) of isobutylene at a TOS less than 10 min, as compared to that for H-FER (14%). Yields of isobutylene for H-S33 are then much lower than those for H-FER after 10 min TOS. Improvement of selectivity to isobutylene for H-S33 only persists for 5 h TOS. In addition, selectivities to isobutylene for H-S33 are smaller than those for H-S22.

2. Steaming of Na/K-FER materials followed by NH_4^+ ion exchange. Na/K-FER was steamed at different temperatures and steam pressures. The steamed products were then ion exchanged with NH_4^+ ions to yield the sample series called NH_4-S. Figures 7Y and 7S illustrate yields and selectivities for *n*-butene skeletal isomerization, respectively, on catalysts NH_4-S11 and NH_4-S33 along with the fresh

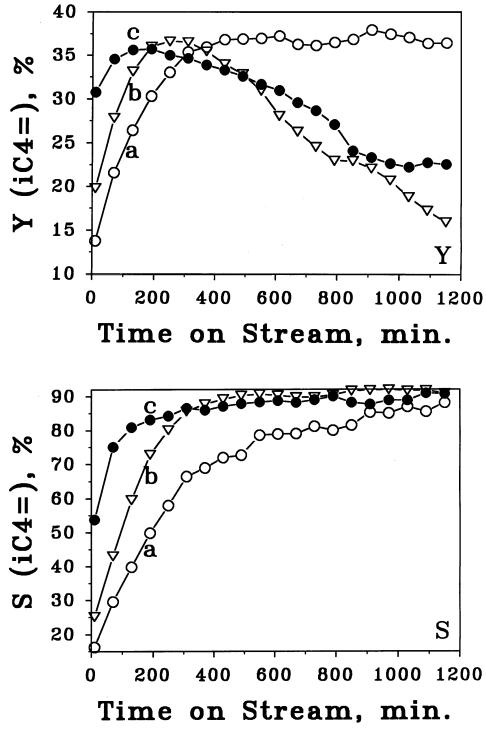

FIG. 7. Yields (Y) and selectivities (S) for *n*-butene skeletal isomerization at a temperature of 693 K and a 1-butene space velocity of 5.34 WHSV on fresh and steamed Na/K-FER materials followed by NH_4^+ ion exchange. (a) NH_4-FER, (b) NH_4-S11, (c) NH_4-S33.

sample (H-FER). Both NH_4-S11 and NH_4-S33 have greater yields of isobutylene than H-FER at a TOS of 5 h. During the TOS for 3 h, improvement of yields of isobutylene for NH_4-S33 is greater than that for NH_4-S11. However, yields of isobutylene for these two catalysts (NH_4-S11 and NH_4-S33) decrease as the TOS goes beyond 5 h. In contrast, fresh sample (H-FER) has steady yields of isobutylene after 5 h TOS. Overall improvements of selectivities to isobutylene were also observed for the NH_4-S series, Fig. 7S. In addition, NH_4-S33 has greater selectivities than NH_4-S11 for 5 h TOS.

3. Washing of H-FER with 1.4 M HNO_3 aqueous solutions. Catalytic data for acid-washed ferrierite/ZSM-35 (H-FER-A) are plotted in Fig. 8Y (yield of isobutylene) and Fig. 8S (selectivity to isobutylene) along with results for the fresh sample (H-FER). Yields of isobutylene for H-FER-A are significantly enhanced, as compared to those for H-FER. Selectivities to isobutylene are also improved from the beginning of the reaction to the longest experimental TOS (20 h). However, both H-FER-A and H-FER take similar TOS to reach a steady value for the yield of isobutylene. In other words, acid washing of H-FER leads to an overall significant improvement of yields and selectivities for *n*-butene skeletal isomerization with no decrease in initiation time for selective skeletal isomerization of *n*-butene.

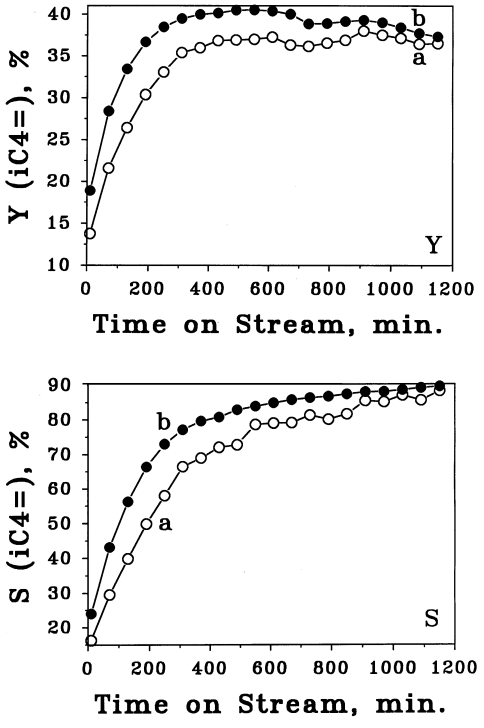

FIG. 8. Yields (Y) and selectivities (S) for *n*-butene skeletal isomerization at a temperature of 693 K and a 1-butene space velocity of 5.34 WHSV on (a) H-FER, (b) H-FER-A.

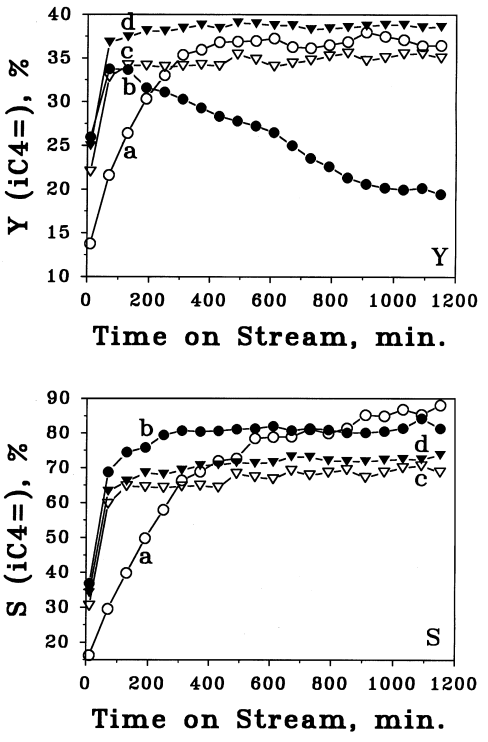

FIG. 9. Yields (Y) and selectivities (S) for *n*-butene skeletal isomerization at a temperature of 693 K and a 1-butene space velocity of 5.34 WHSV on steamed/acid-washed/ion-exchanged ferrierite/ZSM-35 materials. (a) H-FER, (b) H-S22, (c) H-S22-A, (d) H-S22-AM.

4. Acid washing and NH_4^+ ion exchange of H-S series. Mildly steamed H-FER such as H-S11 did not show any improvements of yields and selectivities for *n*-butene skeletal isomerization, as compared to H-FER. Harshly steamed H-FER samples such as H-S22 and H-S33 have shown certain improvements of yields and selectivities for *n*-butene skeletal isomerization at short TOS. However, such harshly steamed H-FER samples are not stable for yields of isobutylene as TOS increases. On the other hand, acid washing of H-FER has shown an overall improvement on yields and selectivities for *n*-butene skeletal isomerization. Therefore, acid-washing of H-S22 was also conducted to yield sample H-S22-A. H-S22-A has very stable yields (35%) and selectivities (65%) right after 1 h TOS, as shown in Figs. 9Y and 9S, respectively. H-S22 was also ion exchanged with 1 *M* NH_4NO_3 to produce H-S22-AM. Higher yields (39%) and selectivities (70%) for *n*-butene skeletal isomerization are also observed for H-S22-AM in addition to excellent catalytic stabilities of yields and selectivities to isobutylene.

5. Acid washing of NH_4-S series. Steaming of Na/K-FER followed by ion exchange with 1 *M* NH_4NO_3 led to improvements of yields of isobutylene up to 5 h TOS. After 5 h TOS, yields of isobutylene reach a maximum and then decrease. On the other hand, acid washing of H-FER has led to an overall improvement of yields and selectivities

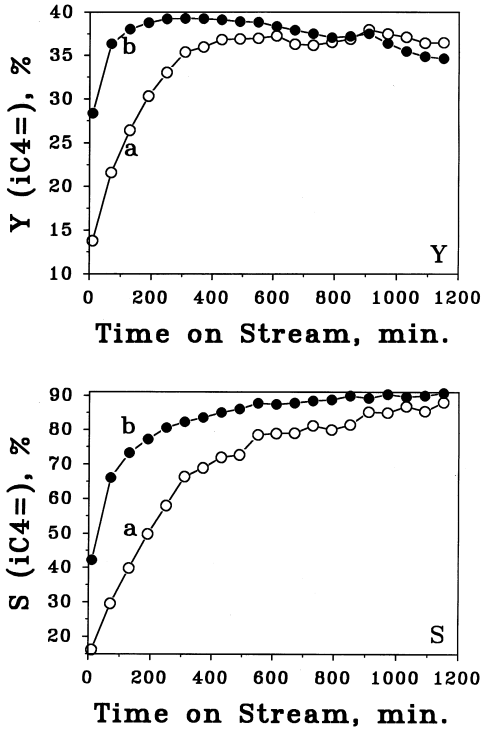

FIG. 10. Yields (Y) and selectivities (S) for *n*-butene skeletal isomerization at a temperature of 693 K and a 1-butene space velocity of 5.34 WHSV on (a) H-FER, (b) NH_4-S31-A.

for *n*-butene skeletal isomerization. Therefore, the NH_4-S series was also washed with 1.4 *M* HNO_3. Figures 10Y and 10S show typical catalytic results for NH_4-S31-A along with H-FER. At TOS of 10 min, NH_4-S31-A has a yield of isobutylene of 28% which is much greater than that for H-FER (14%). Yields of isobutylene after 1 h TOS then reach 36% or greater. Improvement in selectivities to isobutylene for NH_4-S31-A is also very significant. Selectivity to isobutylene at TOS of 10 min is improved from 16 to 42% by such modification. At TOS of 1 h selectivity to isobutylene is greatly improved to about 68%. After a TOS of 1 h, it gradually increases to about 90%.

IV. DISCUSSION

A. *Framework Dealumination of Ferrierite/ZSM-35 Materials by Steaming*

Both H-FER and Na/K-FER materials were steamed at different temperatures (823, 923, and 1023 K) and under different partial pressures of steam (6.67×10^3, 1.33×10^4, and 2.66×10^4 Pa). Crystallinity of these materials decreased due to partial structure collapse during steaming, as suggested by the diffraction intensities of XRD patterns. Indexing of XRD peaks and calculation of lattice parameters of these ferrierite/ZSM-35 materials allow semi-quantitative comparison of the unit cell volumes between these samples, see Table 5. Contraction of the unit cell of ferrierite/ZSM-35 was observed due to framework dealumination. Higher steaming temperature or higher steam pressure leads to a greater contraction for the ferrierite/ZSM-35 unit cell.

The hydrogen form of ferrierite/ZSM-35 favors framework dealumination by steaming over that of sodium/potassium forms (Table 5). Greater contraction of unit cell volumes is observed for the hydrogen form of steamed ferrierite/ZSM-35 than for steamed Na/K-FER materials of NH_4^+ form. For example, contraction of the ferrierite unit cell is about 1.8% for H-S33 which was obtained by steaming H-FER at 1023 K and 2.66×10^4 Pa for 2.5 h. However, only about 0.44% unit cell contraction was observed for sample NH_4-S33 which was obtained by steaming Na/K-FER at 1023 K and 2.66×10^4 Pa for 2.5 h followed by NH_4^+ ion exchange.

Framework dealumination of ferrierite/ZSM-35 materials by steaming is also suggested by ^{27}Al NMR studies. Tetrahedral aluminum ions inside the framework of ferrierite/ZSM-35 have an NMR resonance at about 54 ppm. While extraframework aluminum ions with coordination numbers of 6 and 5 show NMR resonances at −2 and 25 ppm, respectively. A typical ^{27}Al single-pulse MAS NMR spectrum for steamed ferrierite/ZSM-35 materials, H-S22, is shown in Fig. 2b along with that for the fresh sample (Fig. 2a). The ratio of the amount of tetrahedral aluminum ions to that of octahedral ions for H-S22 is about 9 : 5 which is lower than that for the fresh sample (25 : 1). This suggests that steaming has removed some tetrahedral aluminum ions from the framework of ferrierite/ZSM-35 zeolite to form extraframework aluminum ions with a coordination number of 6.

Removal of tetrahedral aluminum ions from the framework of ferrierite/ZSM-35 also leads to a decrease in the intensity of Q_4 Si$(OSi)_3(OAl)$ in ^{29}Si single pulse MAS NMR spectra. The intensity of Q_4 Si$(OSi)_3(OAl)$ at −105 ppm (relative to that of Q_4 Si$(OSi)_4$ at −111 ppm) is reduced by a factor of 50% for H-S22 (Fig. 1c), as compared to that for

TABLE 5

Unit Cell Volumes for Different Steamed Ferrierite/ZSM-35 Materials

Sample	Vu.c., Å^3	Sample	Vu.c., Å^3
H-FER	2038	H-FER	2038
H-S11	2033	NH_4-S11	2032
H-S12	2029	NH_4-S12	2033
H-S13	2032	NH_4-S13	2032
H-S21	2019	NH_4-S21	2033
H-S22	2017	NH_4-S22	2035
H-S23	2010	NH_4-S23	2034
H-S31	2012	NH_4-S31	2033
H-S32	2003	NH_4-S32	2028
H-S32	2006	NH_4-S33	2029

H-FER (Fig. 1a). Such dealumination by steaming creates some defect silicon sites in the steamed ferrierite/ZSM-35 materials, which is suggested by two NMR resonances at −111 and −114 ppm in ^{29}Si cross polarization MAS NMR spectra (Fig. 1b). Steam dealumination may also lead to formation of some extraframework silicon species, detected by NMR resonances at −116 ppm (Fig. 1c).

B. Effects of Steam Dealumination on Acidity of Ferrierite/ZSM-35

1. Steaming of ferrierite/ZSM-35 materials of hydrogen form. Dealumination reduces the number of acid sites for steamed ferrierite/ZSM-35 materials of hydrogen form (H-S series). The higher the steaming temperature or the higher the steam pressure, the smaller the peak areas of IR bands at 3609 cm^{-1} corresponding to Brønsted acid sites (Fig. 3 and Table 2) and 1540 cm^{-1} corresponding to pyridinium chemisorbed on Brønsted acid sites (Fig. 4). Quantitative determination of acid sites by ammonia TPD in Table 4 also suggests that the amount of acid sites in ferrierite/ZSM-35 materials is reduced by steam dealumination. The degree of decrease in the amount of acid sites for steamed ferrierite/ZSM-35 materials depends on temperature and steam pressure. The higher the steaming temperature or the higher the steam pressure, the more acid sites are removed from the ferrierite/ZSM-35 materials due to framework dealumination.

On the other hand, the strength of acidity for ferrierite/ZSM-35 materials is also reduced by steam dealumination. The IR band at 3609 cm^{-1} gradually shifts to new bands at about 3649 cm^{-1} with increasing severity of steaming. These new bands are due to OH bonds corresponding to Brønsted acid sites which are weaker (23) than those corresponding to the IR band at 3609 cm^{-1}. As a reviewer pointed out, such OH groups are created by the detritus of aluminum which is lost from the zeolite framework by steaming. Pyridine chemisorption also shows an infrared band at 1450 cm^{-1} which is characteristic of lewis acid sites. The peak area at 1450 cm^{-1} increases to a maximum and then decreases in the sample series from H-FER to H-S33. These data suggest that some of the strong Brønsted acid sites in the framework are converted into Lewis acid sites. Some of these Lewis acid sites are finally removed from the framework. Therefore, defect silicon sites or silanol nests are created. Generation of silanol nests in steamed ferrierite/ZSM-35 materials is observed by a increase in the IR band at 3742 cm^{-1} (Fig. 3). The presence of defect silicon sites in steamed ferrierite/ZSM-35 materials is also suggested by two NMR resonances at −111 and −114 ppm in the ^{29}Si cross polarization MAS NMR spectrum of Fig. 1b.

Quantitatively, steaming increases the ratio of the amount of weak acid sites to that of strong acid sites. Ferrierite/ZSM-35 materials have both strong and weak acid sites corresponding to two peaks of ammonia desorption at high and low temperatures, Fig. 4. Total amounts of ammonia uptakes are decreased as temperature or steam pressure increases (Fig. 4 and Table 4). The ratio of the amount of strong acid sites to that of weak acid sites increases with the total amount of acid sites in steamed ferrierite/ZSM-35 materials, Fig. 11. These results suggest that steaming removes more strong acid sites than weak acid sites under the same steaming conditions. In other words, the greater the dealumination for steamed ferrierite/ZSM-35 materials, the more strong acid sites are removed (as compared to the removal of weak acid sites).

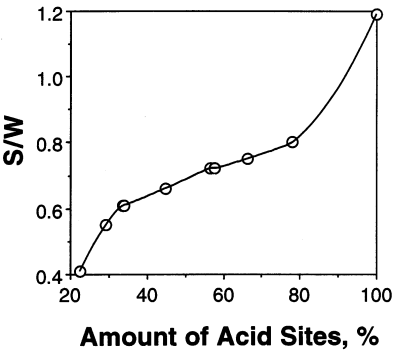

FIG. 11. Correlation of the total amount of acid sites on steamed H-S series (relative to H-FER) with the ratio of the amount of strong acid sites to that of weak acid sites (S/W) determined by ammonia TPD.

2. Steaming of Na/K-FER materials followed by NH_4^+ ion exchange. The presence of sodium and potassium ions in the ferrierite/ZSM-35 materials gives more resistance to steam dealumination. Contraction of the volume of the ferrierite/ZSM-35 unit cell for the NH_4-S series is less than that for the H-S series, Table 5. Ammonia TPD results (Fig. 5) also suggest that there is more ammonia uptake for the NH_4-S series than that of the H-S series (Fig. 4), summarized in Table 4. These results are consistent with those for steaming of zeolite Y of hydrogen and sodium forms (24). In addition, steam pressure seems to have greater effects on dealumination for Na/K-FER materials than steaming temperature when it is below 923 K. Ammonia uptake for ferrierite/ZSM-35 materials (NH_4-S series) decreases with an increase in steam pressure (6.67×10^3, 1.33×10^4, and 2.66×10^4 Pa), but it is very similar for samples steamed at temperatures of 823 and 923 K (Table 4).

The presence of sodium/potassium ions leads to equivalent removal of strong and weak acid sites by steam treatment, Table 5. Ratios of the amounts of strong acid sites to those of weak acid sites are very constant at about 1.18, no matter what steaming conditions were used. In contrast, more strong acid sites are removed from ferrierite/ZSM-35 of hydrogen form than weak acid sites, Table 4. Therefore, the presence of sodium/potassium ions may have protection effects that keep the local zeolite structure more intact during steam dealumination.

C. Acid-washing of Ferrierite/ZSM-35 Materials

Acid washing of H-FER removes some framework aluminum ions on the external surface of ferrierite/ZSM-35 materials. H-FER was washed with 1.4 *M* HNO_3 at 353 K for 12 h to yield sample H-FER-A. XPS analysis shows that the ratio of silicon to aluminum for the surface is increased from 6.0 for H-FER to 7.8 for H-FER-A, a 20% removal of aluminum by acid washing. However, only a 4.9% decrease in the ammonia uptake due to acid washing is detected by ammonia TPD which is mostly due to removal of strong acid sites. ICP analyses also support the results of ammonia TPD experiments. Therefore, one can conclude that acid washing most probably removes aluminum ions on the external surface of ferrierite/ZSM-35 materials, if one framework aluminum ion is assumed to be responsible for one acid site.

Extraframework aluminum ions with octahedral environments (in H-S22) are generated by steaming and show an NMR resonance at −2 ppm, Fig. 2b. Such extraframework aluminum ions still exist in sample H-S22-A even though it was washed with 1.4 *M* HNO_3, as suggested by the NMR resonance at −2 ppm in Fig. 2c. Some of the octahedral (O_h) extraframework aluminum ions are reduced to 5 coordination (an NMR resonance at 25 ppm). Results of ICP analyses also suggest that there are no significant changes in ratios of silicon to aluminum between steamed and acid-washed steamed samples, such as between H-S22 and H-S22-A. On the other hand, the ratio of silicon to aluminum on the external surface of steamed ferrierite/ZSM-35 materials (analyzed by XPS) is increased from 6.0 for H-S22 to 8.0 for H-S22-A, a 22% removal of aluminum ions. These results (NMR, ICP and XPS) suggest that extraframework aluminum ions inside the channels of ferrierite/ZSM-35 can not be removed by acid washing, which is consistent with literature reports (25, 26).

The 5% increase in the amount of acid sites for H-S22-A and H-S22-AM, as compared to H-S22, is probably due to those un-exchangeable Na^+/K^+ ions which remained in the fresh H-FER sample. Such unexchangeable Na^+/K^+ ions in H-FER become available for NH_4^+ exchange after steaming. There actually are about 3.0% of total acid sites potentially available for sample H-FER due to its unexchangeable Na^+ (0.05 wt%) and K^+ ions (0.12 wt%). Therefore, the amount of newly generated acid sites (5% detected) is believed to match well with the amount of unexchangeable Na^+/K^+ ions (3% expected).

D. Skeletal Isomerization of n-Butene to Isobutylene

Out previous research (8) has shown that template-synthesized ferrierite/ZSM-35 materials are better than non-template synthesized ferrierite/ZSM-35 materials in terms of catalytic stability. The non-template synthesized ferrierite/ZSM-35 catalyst needs about 5 h time on stream to achieve a yield of isobutylene of 35%, Fig. 6Ya. Even longer time on stream (14 h) is needed to obtain a selectivity to isobutylene of more than 80%, Fig. 6Sa. The template-synthesized ferrierite/ZSM-35 catalyst only takes about one hour to achieve the same level of yield and selectivity to isobutylene (8). Such differences in catalytic performances occur because non-template synthesized ferrierite/ZSM-35 materials are of lower crystallinity, as compared to their template-synthesized counterparts.

Acid sites which are located inside the large pores (as compared to the zeolitic pores) or on the external surface of non-template synthesized ferrierite/ZSM-35 are responsible for lower shape selectivity at shorter times on stream. Yields and selectivities for isobutylene are improved as time on stream increases, due to coke deposition that poisons strong acid sites and partially blocks the space around non-shape selective acid sites (6), Figs. 6Ya and 6Sa, respectively. Therefore, modification of these non-template synthesized materials causes removal of non-shape selective acid sites in order to achieve more efficient skeletal isomerization of *n*-butene to isobutylene. Another approach for achieving better selectivity to isobutylene involves reducing the number of acid sites to decrease the possibility of interactions of butene intermediates on adjacent acid sites.

1. Removal of non-shape selective acid sites. The non-shape selective acid sites inside the larger pores (as compared to the zeolitic pores) or on the external surface of ferrierite/ZSM-35 has been selectively removed by acid washing, which is suggested by XPS, ICP, and ammonia TPD studies. The catalytic results for such acid-washed ferrierite/ZSM-35 have shown that both yields (Fig. 8Ya) and selectivities to isobutylene (Fig. 8Sa) are enhanced significantly, as compared to those for fresh H-FER (Figs. 8Yb and 8Sb, respectively). However, improvement of the catalytic stability (i.e., initial time) is not significant.

2. Decreasing the number of acid sites. Steaming of ferrierite/ZSM-35 materials leads to framework dealumination so that the number of acid sites is decreased. However, improvement of yields and selectivities to isobutylene for the H-S series (obtained by steaming of ferrierite/ZSM-35 of hydrogen form) is only limited to the first several hours time on stream (Figs. 6Y and 6S). Any improvement of yields and selectivities to isobutylene in the first several hours time on stream cannot exceed a yield of 36% and a selectivity of 90%, respectively, at a time on stream of 20 h for fresh H-FER. In addition, yields of isobutylene for ferrierite/ZSM-35 materials (H-S22 and H-S33) are decreased as time on stream increases. The catalytic stability for the H-S series is not improved.

Improvement of selectivities to isobutylene for the NH_4-S series (obtained by steaming of ferrierite/ZSM-35 of sodium/potassium forms and followed by NH_4^+ ion exchange) is significant as time on stream increases (Fig. 7S). However, improvement of yields of isobutylene is only

limited to the first 5 h time on stream (Fig. 7Y). Yields of isobutylene decrease as time on stream increases (after 5 h). This suggests that catalytic stability is also not improved for th NH_4-S series.

3. Combination of decreasing the number of acid sites and removal of non-shape selective acid sites. Modification for ferrierite/ZSM-35 of hydrogen form by steaming followed by acid washing greatly improves the catalytic stability with respect to yields and selectivities to isobutylene. The number of acid sites is decreased and non-shape selective acid sites are removed due to dealumination. In addition, extraframework aluminum ions (generated by steaming) inside channels of the zeolite can not be removed by acid-washing. After 1 h time on stream, yields and selectivities to isobutylene for such modified zeolite (H-S22-A) are stabilized at about 35 and 65%, respectively (Figs. 9Y and 9S). Such stable catalytic performances may be also due to generation of 5% more acid sites by acid washing, since H^+ ions exchange Na^+/K^+ ions which exist in the fresh sample, H-FER. These additional acid sites can also be generated by NH_4^+ ion exchange, which leads to stable yields (39%) and selectivities to isobutylene (70%). However, selectivities to isobutylene of 70% are still not good enough for commercialization.

Steaming of Na/K-FER followed by NH_4^+ ion exchange and acid washing have proven to be valid procedures for modification of non-template synthesized ferrierite/ZSM-35 materials. Yields of isobutylene are greater than 35% after 1 h time on stream for such modified ferrierite/ZSM-35 (NH_4-S32-A), Fig. 10Y. Selectivity to isobutylene at about 1 h time on stream is near 70% and then increases gradually to about 90%, Fig. 10S. These catalytic performances for such modified non-template synthesized ferrierite/ZSM-35 materials are very close to those for template-synthesized ferrierite/ZSM-35 materials (8).

V. CONCLUSIONS

Steaming of non-template synthesized ferrierite/ZSM-35 materials leads to framework dealumination to different degrees, depending on steaming temperature and steam pressure. The higher the steaming temperature or the higher the steam pressure, the more the framework aluminum ions are removed. The presence of Na^+/K^+ ions leads to more resistance to framework dealumination during steaming.

The number of acid sites is decreased by steaming along with framework dealumination. Greater amounts of strong acid sites have been removed for steamed ferrierite/ZSM-35 of hydrogen form, as compared to the removal of weak acid sites. Steaming of ferrierite/ZSM-35 of Na^+/K^+ forms removes an equal number of strong and weak acid sites.

Framework dealumination of ferrierite/ZSM-35 by acid washing only occurs on the surface of the material, suggested by XPS, ICP, and ammonia TPD studies. Acid washing has been proven to be very effective for removal of non-shape selective acid sites. These non-shape selective acid sites are located inside larger pores (as compared to the zeolitic pores) or on the external surface of ferrierite/ZSM-35 materials due to their lower crystallinity (8). In addition, acid washing cannot remove extraframework aluminum ions inside the zeolite channels, as suggested by NMR, XPS, and ICP studies. These extraframework aluminum ions are generated during framework dealumination by steaming.

Kinetic studies of skeletal isomerization of *n*-butene to isobutylene have shown that steaming of ferrierite/ZSM-35 of Na^+/K^+ forms followed by NH_4^+ ion exchange and acid washing is a very effective method for modification of non-template synthesized ferrierite/ZSM-35 materials. Catalytic performances for such modified materials are very close to those for template-synthesized ferrierite/ZSM-35 materials, with respect to yields, selectivities, and stability. Improvements in catalytic performances via such modification procedures are basically due to two factors: (1) removal of non-shape selective acid sites suppresses butene dimerization and its sequential side reactions, and (2) lowering of the number of acid sites decreases interactions between butene intermediates located in adjacent acid sites.

ACKNOWLEDGMENTS

The authors thank the Office of Basic Energy Sciences, Division of Chemical Sciences, Department of Energy and Texaco, Inc., for support of this research. The authors appreciate Dr. William Willis for his help in XPS analysis. Mr. Alexander Yuzefovsky and Mr. Noel Miraflor are also appreciated for their help in ICP experiments.

REFERENCES

1. Pecci, G., and Floris, T., *Hydrocarbon Process.* **56** (12), 98–102 (1977).
2. Xu, W.-Q., Suib, S. L., and O'Young, C.-L., *J. Catal.* **144**, 285–295 (1993).
3. Simon, M. W., Nam, S. S., Xu, W.-Q., Suib, S. L., Edwards, J. C., and O'Young, C.-L., *J. Phys. Chem.* **96**, 6381–6388 (1992).
4. Simon, M. W., Xu, W.-Q., Suib, S. L., and O'Young, C.-L., *Microporous Mater.* **2**, 447–486 (1994).
5. Bianchi, D., Simon, M. W., Nam, S. S., Xu, W.-Q., Suib, S. L., and O'Young, C.-L., *J. Catal.* **145**, 551–560 (1994).
6. Xu, W.-Q., Yin, Y.-G., Suib, S. L., and O'Young, C.-L., *J. Phys. Chem.* **99**, 758–765 (1995).
7. U.S. Patent 5,227,569, assigned to Texaco, Inc.
8. Xu, W.-Q., Yin, Y.-G., Suib, S. L., Edwards, J. C., and O'Young, C.-L., *J. Phys. Chem.* **99**, 9443–9451 (1995).
9. Xu, W.-Q., Yin, Y.-G., Suib, S. L., and O'Young, C.-L., *J. Catal.* **150**, 34–45 (1994).
10. Simon, M. W., Suib, S. L., and O'Young, C.-L., *J. Catal.* **147**, 484–493 (1994).
11. Vaughan, P. A., *Acta Crystallogr.* **21**, 983–990 (1966).
12. Marosi, L., Schwarzmann, M., and Stabenow, J., European patent 49,386, April 14, 1982.
13. Hellring, S. D., Chang, C. D., and Luther, J. D., U.S. Patent 5,190,736, March 2, 1993.
14. Plank, C. J., Rosinski, E. J., and Rubin, M. K., U.S. Patent 4,046,859, Sept. 6, 1977.

15. Nanne, J. M., Post, M. F. M., and Stork, W. H. J., European Patent 12,473, June 25, 1980.
16. Suzuki, K., Kiyozumi, Y., Shin, S., Fujisawa, K., Watanabe, H., Saito, K., and Noguchi, K., *Zeolite* **6**, 290–298 (1986).
17. Dutta, P. K., Rao, K. M., and Park, J. Y., *Langmuir* **8**, 722–726 (1992).
18. Whittam, T. V., European Patent 103,981, March 28, 1984.
19. Inaoka, W., Kasahara, S., Fukushima, T., and Igawa, K., *in* "Synthesis and Characterization of Zeolites" (T. Inui, S. Namba, and T. Tatsumis, Eds.), *Stud. Surf. Sci. Catal.*, Vol. 60, 1991, p. 37.
20. Xu, W.-Q., and Suib, S. L., *J. Catal.* **145**, 65–72 (1994).
21. Messner, A. E., Rosie, D. M., and Argabright, P. A., *Anal. Chem.* **31**, 230–233 (1959).
22. Rosie, D. M., *Anal. Chem.* **29**, 1263–1264 (1957).
23. Chu, C. T.-W., and Chang, C. D., *J. Phys. Chem.* **89**, 1569–1571 (1985).
24. Szostak, R., in Introduction to Zeolite Science and Practice; H. v. Bekkum, (E. M. Flanigen and J. C. Jansen, Eds.), Vol. 58; p. 153. Elsevier, 1991.
25. Jin, Y. S., Auroux, A., and Vedrine, J. C., *Appl. Catal.* **37**, 1–19 (1988).
26. Jin, Y. S., Auroux, A., and Vedrine, J. C., *Appl. Catal.* **37**, 21–33 (1988).